

Initiating gradient photopolymerization and migration of a novel polymerizable polysiloxane α -hydroxy alkylphenones photoinitiator



Fang Sun ^{a, b, *}, Yanxia Li ^b, Nan Zhang ^b, Jun Nie ^{a, c}

^a State Key Laboratory of Chemical Resource Engineering, Beijing University of Chemical Technology, Beijing 100029, PR China

^b College of Science, Beijing University of Chemical Technology, Beijing 100029, PR China

^c College of Materials Science and Engineering, Beijing University of Chemical Technology, Beijing 100029, PR China

ARTICLE INFO

Article history:

Received 23 January 2014

Received in revised form

30 May 2014

Accepted 14 June 2014

Available online 21 June 2014

Keywords:

Gradient polymerization

Polymerizable organosilicon photoinitiator

Migration

ABSTRACT

This paper reported a photocleavage type polymerizable organosilicon macromolecular photoinitiator (HHMP-Si-CC), which was synthesized based on traditional photoinitiator 2-hydroxy-1-[4-(2-hydroxyethoxy) phenyl]-2-methyl propan-1-one (HHMP) and amino polysiloxane. HHMP-Si-CC cannot only spontaneously form a concentration gradient in the photopolymerization system, initiate gradient photopolymerization and effectively mitigate inhibition of oxygen, but also overcome the migration of photolysis fragments of the photoinitiator from UV-curable material. Its structure was confirmed by proton nuclear magnetic resonance (¹H NMR), ¹³C NMR, ²⁹Si NMR and Fourier transform infrared spectroscopy (FTIR) and gel permeation chromatography (GPC). The kinetics of photopolymerization of HHMP-Si-CC was studied by real-time infrared spectroscopy (RTIR). Moreover, it was proved by X-ray photoelectron spectroscopy (XPS) and UV absorption that HHMP-Si-CC had relatively good self-floating ability. The polymer initiated by HHMP-Si-CC presented a gradient change in the degree of polymerization, molecular weight, thermostability and glass transition temperature (T_g). The surface morphology of poly(triethylene glycol diacrylate) (PTPGDA) initiated by HHMP-Si-CC was studied by scanning electron microscopy (SEM). More importantly, the migration of photolysis fragments of the HHMP-Si-CC from UV-curable materials was also investigated by high performance liquid chromatography (HPLC). The results showed that the migration more was effectively mitigated by introducing polymerizable groups into the HHMP-Si-CC. HHMP-Si-CC should have potential applications for preparing more environmentally friendly gradient materials.

© 2014 Elsevier Ltd. All rights reserved.

1. Introduction

Over the past few years, polymeric gradient materials (PGM) [1–3] possessing a gradient in composition, microstructure and property have attracted much attention for investigating the effects of variation on multiple parameters [4]. PGM exhibit spatial variations in structure and/or composition, which have been imposed to obtain unprecedented properties and functionalities that cannot be realized in homogeneous materials. The use of PGM is continuously growing in industry as reflected by many applications in not only aerospace, energy, electronics, medical but also optical and other industries [5]. With the increased attention from researchers, a wide range of process technologies including changing light

intensity [6], applying gradient temperature field [7] or gradient solution concentration [8], and utilizing magnetic separation [9], are now available for preparing PGM. However, these techniques have limitations because of multiple steps, thereby increasing cost and pollution to environment and decreasing convenience. Therefore, the development of a simpler, more environmentally friendly and convenient method for preparing PGM has been a focus of much research in recent years.

We have proposed a fast, convenient and environmentally friendly method to prepare molecular weight gradient polymer by using a polysiloxane benzophenone photoinitiators with good self-floating ability, leading to the spontaneous formation of a concentration gradient of the photoinitiator in a photopolymerization system. Our previous work [10] reported the effect of silicone chain length of the polysiloxane benzophenone photoinitiators on the self-floating ability of the photoinitiator, and the microstructure and surface property of the molecular weight gradient polymer, however, the research on the gradient distribution of the degree of

* Corresponding author. College of Science, State Key Laboratory of Chemical Resource Engineering, Beijing University of Chemical Technology, PO Box 144, Beijing 100029, PR China. Tel.: +86 10 64449336; fax: +86 10 64437802.

E-mail address: sunfang60@yeah.net (F. Sun).

the photopolymerization initiated by the polysiloxane-based photoinitiator and properties of the obtained gradient polymer, and their internal connection were not involved. The research is very important to prepare an expected gradient polymer. It is notable that the reported polysiloxane-based photoinitiators are a hydrogen-abstraction type photoinitiator system (Norish type II) that has drawbacks of yellowing, toxicity and mutagenicity derived from coinitiator amines [11–14]. Therefore, the photocleavage type (Norish type I) polysiloxane-based photoinitiators that produce two radicals through an unimolecular cleavage to initiate polymerization have been expected as good alternatives. Additionally, when photoinitiators initiate polymerization, their photolysis fragments and unreacted molecules might diffuse from UV-cured materials, resulting in an impact on human health and environment. One important method to solve the problem is the introducing polymerizable groups into photoinitiator molecules [15–17], which can be polymerized into the polymer backbone.

In this work, we reported a novel polymerizable photocleavage polysiloxane macromolecular photoinitiator (HHMP-Si-CC) that overcame some drawbacks of the hydrogen-abstraction type polysiloxane-based photoinitiator and the migration of photolysis fragments of photoinitiator from UV-cured materials. The self-floating ability of the photoinitiator was evaluated by the UV absorption spectra and X-ray photoelectron spectroscopy (XPS). The migration of photolysis fragments of the photoinitiator from UV-curable materials was also investigated by high performance liquid chromatography (HPLC). More importantly, the gradient distribution of the degree of the photopolymerization initiated by the photoinitiator and properties of the prepared gradient polymer, and their internal connection were fully discussed.

2. Experimental details

2.1. Materials

Amino polysiloxane (A-Si) ($M_n = 450$, amino equivalent: 225 g mol^{-1}) was from Shin-Etsu Chemical Co. Ltd. (Shanghai, China). 2-hydroxy-1-[4-(2-hydroxyethoxy) phenyl]-2-methyl propan-1-one (HHMP), N,N-dimethylaniline, triethanolamine (TEOA), p-toluenesulfonyl chloride (TsCl), N, N-dimethylformamide (DMF), potassium carbonate (K_2CO_3), potassium hydroxide (KOH), methylene chloride (CH_2Cl_2), 3-bromopropene and ethyl acetate were purchased from Sinopharm Group Chemical Reagent Co. (Beijing, China). Tripropylene glycol diacrylate (TPGDA) and methyl methacrylate (MMA) monomers were purchased from Eternal Chemical Co. Ltd. (Tianjin, China). All reagents were used as received without further purification.

2.2. Synthesis of polysiloxane photoinitiator HHMP-Si-CC

2.2.1. Synthesis of HHMP-S

HHMP (26.9 g, 0.12 mol), TsCl (19.0 g, 0.10 mol) and KOH (22.4 g, 0.40 mol) were dissolved in 300 mL of CH_2Cl_2 in a 500 mL three-necked round bottom flask, which was equipped with a

mechanical stirrer and a condenser. The solution was stirred at ambient temperature ($25 \text{ }^\circ\text{C}$) for 2 h and then washed three times with deionized water. The organic layer was dried over Na_2SO_4 , and filtered, then distilled under vacuum. The crude product was purified by silica gel (200–300 mesh) column chromatography using ethyl acetate and methylene chloride (1:20v/v) as an elution and the yield was 62.5%. The synthesis process is shown in Scheme 1.

FTIR (KBr, cm^{-1}): 3456 cm^{-1} (–OH), 3062 cm^{-1} (=C–H), 2984 cm^{-1} , 2865 cm^{-1} (–CH₃, –CH₂), 1663 cm^{-1} (>C=O), 1598 cm^{-1} , 1445 cm^{-1} (–C₆H₅), 1359 cm^{-1} (–SO₂–), 1250 cm^{-1} , 1020 cm^{-1} (Ar–O–C).

¹H NMR (400 MHz, CDCl_3 , ppm): 8.03, 7.82, 7.35, 6.84 (Ar–H), 4.42–4.40 (CH_2CH_2), 2.45 (ArCH₃), 1.62 (CH_3CCH_3).

2.2.2. Synthesis of NH_2 -HHMP

HHMP-S (13.7 g, 0.04 mol), A-Si (9.0 g, 0.02 mol) and K_2CO_3 (19.9 g, 0.14 mol) were dissolved in 300 mL of DMF in a 500 mL four-necked round bottom flask, which was equipped with a mechanical stirrer, a thermometer and a condenser. The solution was stirred at $110 \text{ }^\circ\text{C}$ for 24 h. The product was washed three times with 10% NaOH aqueous solution and deionized water, respectively. The solvent was removed by vacuum distillation. Then the crude product was purified by silica gel (200–300 mesh) column chromatography using ethyl acetate and hexane (1:4v/v) as an elution. The yield was 58.7%. The molecular weight measured by GPC was about 897. The synthesis process is shown in Scheme 2.

FTIR (KBr, cm^{-1}): 3342 cm^{-1} (–OH, –NH), 3068 cm^{-1} (=C–H), 2959 cm^{-1} , 2875 cm^{-1} (–CH₃, –CH₂), 1661 cm^{-1} (>C=O), 1594 cm^{-1} (–C₆H₅), 1374 cm^{-1} (–CH₃), 1033 cm^{-1} (Si–O–Si), 1253 cm^{-1} and 798 cm^{-1} (Si–CH₃).

¹H NMR (400 MHz, CDCl_3 , ppm): 8.08, 6.96 (Ar–H), 3.05–4.17 (CH_2CH_2), 1.64 (CH_3CCH_3), 0.09 (SiCH₃).

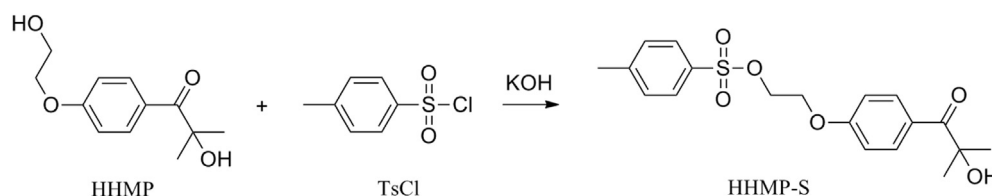
2.2.3. Synthesis of HHMP-Si-CC

NH_2 -HHMP (0.62 g, 0.68 mmol), 3-bromopropene (0.33 g, 2.72 mmol) and K_2CO_3 (1.88 g, 13.60 mmol) were dissolved in 20 mL of acetone in a 100 mL three-necked round bottom flask, which was equipped with a mechanical stirrer, a thermometer and a condenser. The solution was refluxed at $70 \text{ }^\circ\text{C}$ for 12 h and washed three times with deionized water. The organic layer was dried over Na_2SO_4 , and filtered, then distilled under vacuum. The crude product was purified by silica gel (200–300 mesh) column chromatography using ethyl acetate and hexane (1:4v/v) as an elution and the yield was 47.3%. The molecular weight measured by GPC was about 1073. The synthesis process is shown in Scheme 3.

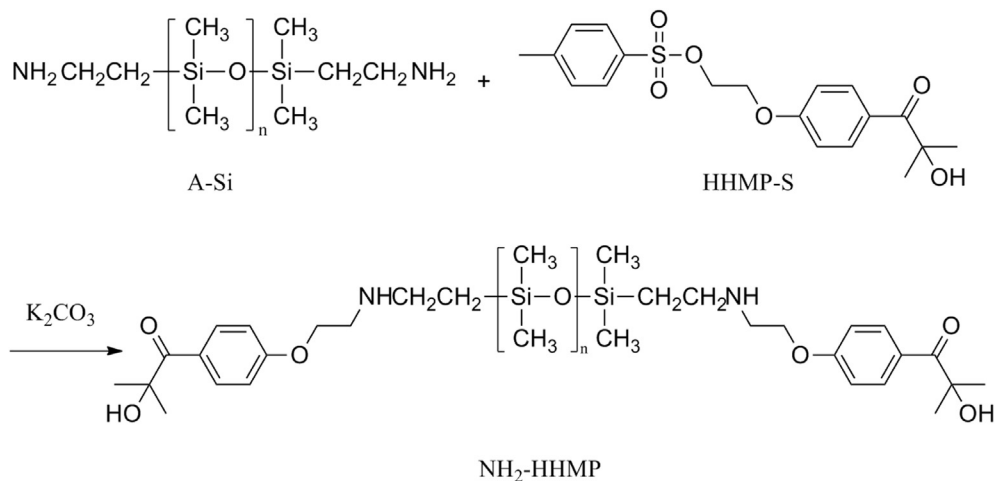
FTIR (KBr, cm^{-1}): 3456 cm^{-1} (–OH), 3079 cm^{-1} (=C–H), 2952 cm^{-1} , 2872 cm^{-1} (–CH₃, –CH₂), 1666 cm^{-1} (>C=O), 1638 cm^{-1} (–C=C–), 1601 cm^{-1} (–C₆H₅), 1373 cm^{-1} (–CH₃), 1033 cm^{-1} (Si–O–Si), 1259 cm^{-1} and 799 cm^{-1} (Si–CH₃).

¹H NMR (400 MHz, CDCl_3 , ppm): 8.08, 6.95 (Ar–H), 6.03–6.10, 5.32–5.47 ($\text{CH}_2=\text{CH}$), 3.90–4.21 (CH_2CH_2), 1.64 (CH_3CCH_3), 0.90 (SiCH₃).

¹³C NMR (400 MHz, CDCl_3 , ppm) δ : 201.5, 161.5, 145.3, 131.4, 125.3, 114.7, 112.9, 75.2, 68.5, 66.5, 59.5, 44.5, 27.4, 14.2, 0.1.



Scheme 1. Synthesis route of HHMP-S.



Scheme 2. Synthesis route of $\text{NH}_2\text{-HHMP}$.

^{29}Si NMR (400 MHz, CDCl_3 , ppm) δ : -22.2 (Si (CH_3) $_2$).

2.3. Synthesis of gradient polymer cylinder initiated by HHMP-Si-CC

HHMP-Si-CC (0.5 wt%, relative to monomers) was dissolved in TPGDA or MMA monomer, then as-prepared solution was added into a vertical glass tube with an inner diameter of 6 mm to form 4 cm fluid column. After standing for 60 min, the fluid column was irradiated with the high-pressure mercury lamp with 365 nm emission wavelength (incident light intensity = 50 mW cm^{-2} , recorded by UV Light Radiometer (Photoelectric Instrument Factory, Beijing Normal University, Beijing, China)). The photoinitiator content, degree of polymerization, molecular weight, glass transition temperature (T_g), and thermostability of different vertical level of the gradient polymer were measured by XPS, Raman spectra, GPC, DSC and TGA.

2.4. Synthesis of gradient polymer film in aerobic conditions

Photoinitiators HHMP ($4.0 \times 10^{-3} \text{ mol L}^{-1}$) and HHMP-Si-CC ($4.0 \times 10^{-3} \text{ mol L}^{-1}$) were dissolved in the TPGDA respectively. A measured volume of the UV-resin formulation was dispensed on a

pre-cleaned glass slide and allowed to spread to a diameter of 20 mm to obtain liquid resin film of desired thickness. After standing for 60 min, the deposited liquid film was then exposed to high-pressure mercury lamp with 365 nm emission wavelength (incident light intensity = 50 mW cm^{-2}) for 60 s in aerobic conditions. After exposure, the uncured liquid layer on top was allowed to swell the bottom gradient film for 20 min to fully develop the wrinkles to obtain the gradient polymer films, which were measured by SEM.

2.5. Characterization methods

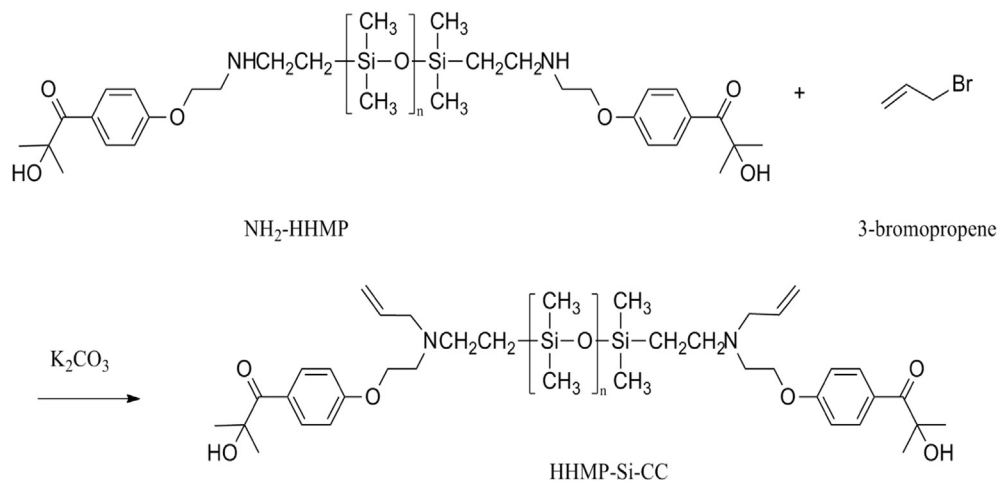
2.5.1. Characterization of the photoinitiator

The Fourier transform infrared (FTIR) spectra were recorded according to a Nicolet 50XC spectrometer (Nicolet, USA) and scanned between 400 and 4000 cm^{-1} .

The ^1H NMR spectra were recorded on an AV400 unity spectrometer (Bruker, Germany) operated at 400 MHz with CDCl_3 as a solvent and tetramethylsilane as an internal standard.

2.5.2. The average molecular weight of the gradient polymer

The average molecular weight of the gradient polymer was determined by GPC (Water 515-2410, USA). Tetrahydrofuran,



Scheme 3. Synthesis route of HHMP-Si-CC.

1.0 mL min⁻¹, was used as the mobile phase. Linear polystyrenes (PS) with various molecular weights were used as the calibration standard.

2.5.3. UV absorption and UV degradation of the photoinitiator

The properties of UV absorption and UV degradation were studied by UV absorption spectroscopy (Hitachi High-Technologies Corporation, Tokyo, Japan) and scanned between 200 and 500 nm.

2.5.4. The surface morphology and elemental composition of the polymer

The surface morphology of the polymer was observed by SEM (S-4700 Hitachi) with an accelerating voltage of 20.0 kV.

The elemental compositions of different vertical levels of the gradient polymer rod (TPGDA) initiated by HHMP-Si-CC were investigated by using XPS (Thermo Electron Corporation, Escalab 250, Germany).

2.5.5. DSC and thermal analysis

Differential scanning calorimetric (DSC) measurements were performed in a nitrogen atmosphere on 5–15 mg polymer samples at a heating rate of 20 °C min⁻¹ using Pyris 1 (Perkin Elmer). Thermogravimetry analysis (TGA) was performed on STA-449C thermogravimetric analysis instrument (NETZSCH Instrument Co., Germany) under a nitrogen atmosphere with a heating rate of 20 °C min⁻¹ in the temperature range of 25–500 °C.

2.5.6. HPLC analysis

The HPLC analysis was performed on an Agilent 1100 series instrument coupled to a variable wavelength detector (VWD). Samples were separated on a C₁₈ column (5 μm, 150 × 4.6 mm i.d.) with a sample injection volume of 25 μL. The mobile phase was mixtures of acetonitrile (A) and water (B). A gradient program was used as follows: 70% A (0 min), 70% A (5 min), 100% A (15 min). The mobile phase flow rate was 1.0 mL min⁻¹. Column temperature was controlled at 25 °C.

2.6. Migration of photoinitiator fragment of photoinitiator from UV-curable film

Photoinitiator HHMP (1.0 × 10⁻³ mol L⁻¹) and HHMP-Si-CC (5.0 × 10⁻⁴ mol L⁻¹) with the same molarity of the photosensitive group were dissolved in the TPGDA respectively. A measured volume of the UV-resin formulation was dispensed on a pre-cleaned glass pane and allowed to spread to a diameter of 20 mm to obtain a liquid resin film of desired thickness, then covered with a cover glass to ensure anaerobic conditions. Subsequently, the deposited liquid film was exposed to the high-pressure mercury lamp with 365 nm emission wavelength (incident light intensity = 10 mW cm⁻²) for 15 min to obtain the cured films. Then 1.0 g of the mashed cured films was extracted with acetonitrile in a Soxhlet extractor for 96 h. The extraction solution was analyzed by HPLC to investigate the migration of photolysis fragment of the

photoinitiator from UV-curable film. The basic concept for our approach is schematically illustrated in Scheme 4.

2.7. Photopolymerization

TPGDA was employed to investigate kinetics of photopolymerizations initiated by HHMP-Si-CC with real-time infrared spectroscopy (RTIR) (Nicolet 5700, Thermo Electron, USA, equipped with an extended range KBr beam-splitter and an MCT/A detector) according to previous reported procedure [10].

2.8. Raman spectra

Raman spectra of different vertical level of PMMA rod mentioned in section 2.3 were collected using a Renishaw InVia reflex Raman microscope to detect degree of photopolymerization. The Raman scattering was excited with a 785 nm near-infrared diode laser. Data acquisition covered the spectral range 3000–120 cm⁻¹ with a spectral resolution of 1.5 cm⁻¹ with each exposure of the CCD detector.

A band whose intensity does not change during polymerization should be selected as a reference band. In this study, the C–H stretching band at 2986 cm⁻¹ was selected as a reference band. It is well known that the C=C stretching mode at 1640 cm⁻¹ can be influenced during polymerization. Then the intensities for the individual bands (2986 and 1640 cm⁻¹) were obtained from the peak areas by the curve fitting software. Care should be taken that the obtained percentages were based on the assumption that the linearity of the ratios between uncured and cured states existed. The percentage of the final double bond conversions (DBC) was calculated using the following equation:

$$\text{DBC}(\%) = (1 - A_{\text{cured}}/A_{\text{uncured}}) \times 100\% \quad (1)$$

where

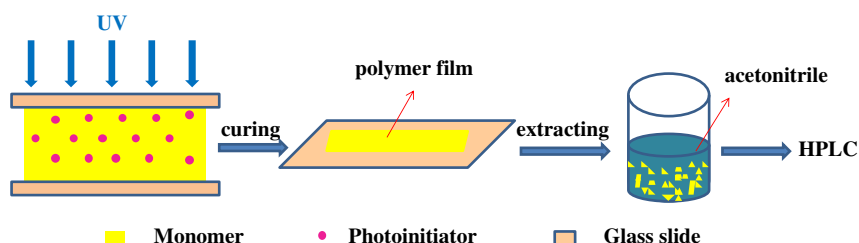
$$A_{\text{cured}} = (\text{C}=\text{C} \text{ absorbance area} / \text{C}-\text{H} \text{ absorbance area})_{\text{cured}}$$

$$A_{\text{uncured}} = (\text{C}=\text{C} \text{ absorbance area} / \text{C}-\text{H} \text{ absorbance area})_{\text{uncured}}$$

2.9. Self-floating ability

The self-floating of the photoinitiator was investigated by UV absorption spectra. The experimental details were as follows.

HHMP-Si-CC was dissolved in absolute ethyl alcohol to obtain homogeneous solution with various concentrations 10⁻² mol L⁻¹, 10⁻³ mol L⁻¹ and 10⁻⁴ mol L⁻¹, and the as-prepared solutions were added into cuvettes to measure the UV absorption. The maximum absorbance of HHMP-Si-CC was obtained from the UV absorption spectra. According to the Lambert–Beer law, the average absorption coefficient (ε) of HHMP-Si-CC was calculated to 2.556 × 10⁴ L mol⁻¹ cm⁻¹. Then HHMP-Si-CC solution with concentration 10⁻³ mol L⁻¹ was added into a vertical glass tube having an inner diameter of 3 cm and depth of 25 cm. After standing at



Scheme 4. Schematic representation of the extraction of the cured film initiated by HHMP and HHMP-Si-CC as a photoinitiator in anaerobic conditions.

various time scales ranging from 0 to 60 min, 1.0 mL aliquots were carefully taken out from top or bottom in the vertical glass tube and put into a 10 mL volumetric flask respectively, and then diluted with 9.0 mL of absolute ethyl alcohol before measuring the UV absorption. With the maximum absorbance of the UV absorption spectra, the concentrations of HHMP-Si-CC in the top layer and the bottom layer at different standing time were calculated according to the Lambert–Beer law.

For comparing, similarly, the concentrations of HHMP in the top layer and the bottom layer at different standing time were calculated according to the above procedure.

3. Results and discussion

3.1. Synthesis and structural characterization of HHMP-Si-CC

With comparison of with the curve of HHMP, the typical absorption peaks of C=C were observed at about 3079 and 1638 cm^{-1} . Characteristic absorption peaks of OH-, >C=O, -C₆H₅, Si-O-Si and Si-CH₃ appear at 3343, 1659, 1594, 1513, 1036 and 1259 cm^{-1} respectively in the curve of HHMP-Si-CC, indicating that HHMP was successfully linked with the A-Si (Fig. 1).

Fig. 2 shows that the signals of aromatic hydrogen of HHMP at 6.9–8.0 ppm and allyl peaks at 5.7–6.1 ppm were observed in the spectrum of HHMP-Si-CC, indicating that A-Si had been linked with HHMP and 3-bromopropene. After a nucleophilic substitution reaction, the chemical shifts of -CH₂CH₂- in HHMP (4.2–4.4 ppm) were shifted upfield (3.9–4.2 ppm) in HHMP-Si-CC due to the effect of N atom. The integration ratio of Si-CH₃ to Si-CH₂ (peak a' in Fig. 2) in HHMP-Si-CC was 7.0, which was similar to the corresponding ratio (7.1) of Si-CH₃ to Si-CH₂ (peak a in Fig. 2) in A-Si, and the integration ratio of H-d' to H-c' in HHMP-Si-CC was 2.0, demonstrating that HHMP and 3-bromopropene linked with both sides of the A-Si. Additionally, integration ratio verified that polymerization degree (*n*) of A-Si was 3–5. Hence, the NMR estimates could deduce the molecular weight of A-Si was 392–540 and HHMP-Si-CC was 889–1037, similar to the GPC results.

3.2. UV/vis absorption degradation properties

The UV absorption spectra of HHMP and HHMP-Si-CC in absolute ethanol are showed in Fig. 3. The maximum absorption peaks of HHMP and HHMP-Si-CC all were at 275 nm and absorption

intensity were also similar due to contain the same molar concentration of chromophore.

The UV/vis degradation curves of HHMP-Si-CC in absolute ethanol are shown in Fig. 4. The results revealed that the intensity of the UV/vis absorption tended to decrease against the increase of the UV irradiation time because of the decomposition of HHMP-Si-CC. Additionally, the π - π^* transition of HHMP-Si-CC underwent a blue-shift after irradiation. It may be due to dealkylation process of HHMP chromophore under UV light irradiation [18].

3.3. Kinetic study of photopolymerization initiated by HHMP-Si-CC

The plots of the double bond conversion vs. time for TPGDA initiated by HHMP-Si-CC and HHMP with the same molar concentration of chromophore are shown in Fig. 5. It was found that HHMP and HHMP-Si-CC had similar photoinitiating activities.

Fig. 6 shows that the polymerization rate and the final double bond conversion increased with the increase of HHMP-Si-CC concentration as more free radicals were produced with the higher concentration of HHMP-Si-CC.

When the light intensity was lower than 30 mW cm^{-2} , the increase in the light intensity resulted in an increase in the polymerization rate and final double bond conversion due to more free radicals produced during irradiation as shown in Fig. 7. However, at a too high light intensity, the polymerization rate and the final double bond conversion were reduced. The possible explanation for the result was the fact that the rapid photodegradation of the photoinitiator led to a lower concentration of propagating radicals due to an increase in the rate of radical–radical combination reactions. At the relatively high light intensities, radical combination reactions could dominate thereby preventing effective polymerization [14].

3.4. Self-floating ability

Fig. 8 shows the HHMP and HHMP-Si-CC concentrations of the top layer and bottom layer of the system undergoing different standing time. With the increase of standing time, the HHMP-Si-CC concentration of the top layer increased, while the concentration of the bottom layer decreased, and they all reached equilibrium at about 50 min, with the migration rate of about 13%. However, the HHMP concentration of the top layer and bottom layer did not vary significantly with the increase of standing time. This result indicated that the HHMP-Si-CC had a relatively good self-floating ability and spontaneously formed a gradient distribution of concentration in the polymerization system.

The abundances of C, O and Si on the surface of each segment from top to bottom layer of polymer rod prepared using HHMP-Si-CC as an initiator were detected (Fig. 9(a)). The content of Si can directly reflect the content of the HHMP-Si-CC since the monomer does not contain Si element. Fig. 9(b) shows that content of Si decreased gradually from the top to the bottom layer. The content of Si on the top layer, the second layer, the third layer and the bottom layer was 14.80%, 8.30%, 5.91% and 3.39%, respectively, which meant that there was a gradient distribution of HHMP-Si-CC from the surface down to the bottom in the polymerization system. Moreover, there was the deviance between the results of UV–vis measurements in Fig. 8 and the XPS analysis, because of the different medium (the ethanol solution and the UV-curable system of TPGDA) and measuring methods.

3.5. Gradient polymerization of PMMA initiated by HHMP-Si-CC

Both the UV and XPS measurements confirmed that there was an uneven radical photoinitiator concentration distribution in the

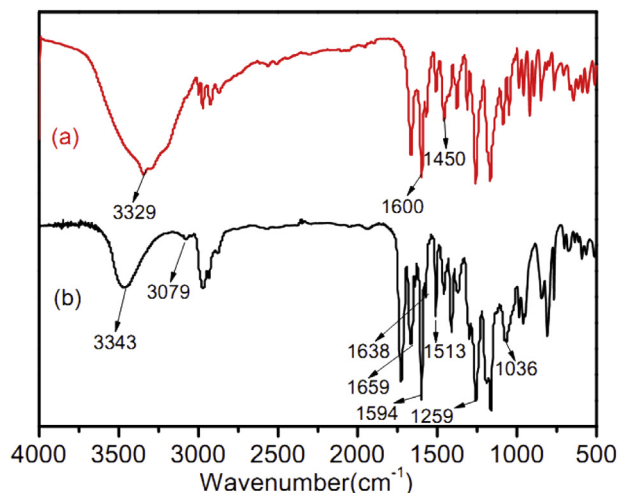


Fig. 1. FTIR spectra for HHMP (a) and HHMP-Si-CC (b).

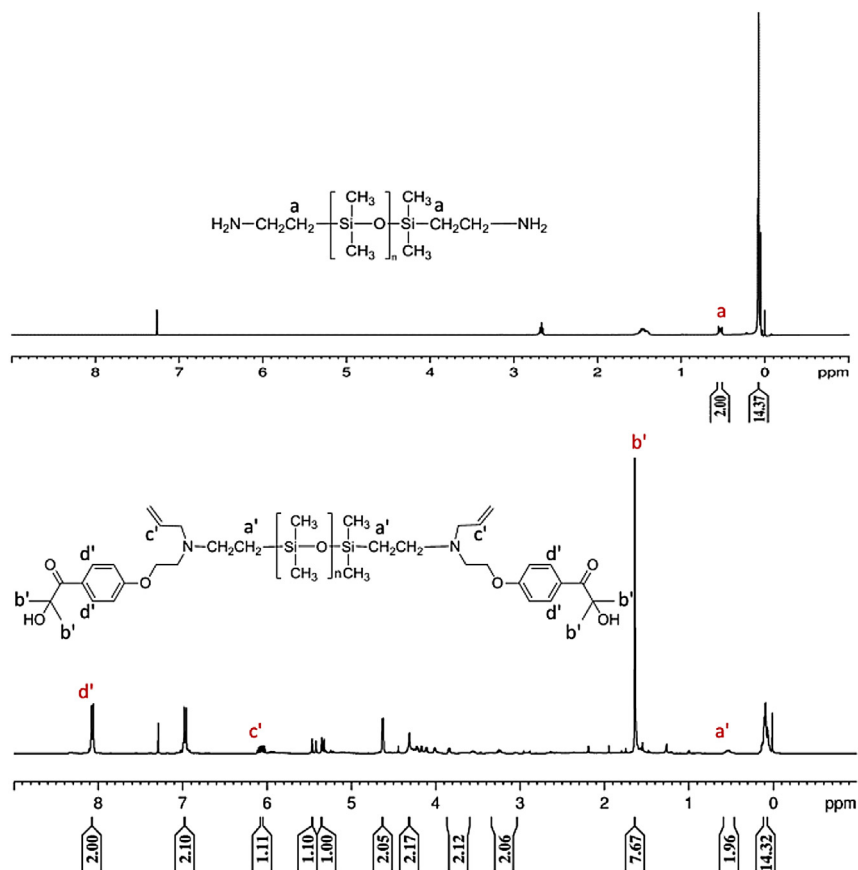


Fig. 2. ^1H NMR spectra of A-Si and HHMP-Si-CC.

photopolymerization system containing HHMP-Si-CC, which will affect degree of photopolymerization of the system, thereby influencing properties of the polymer. The gradient polymerization of the PMMA initiated by HHMP and HHMP-Si-CC was investigated by Raman spectrum (Fig. 10 and Table 1). It was easily found that for HHMP system, DBC presented no clear trend from top layer to bottom layer of PMMA rod, whereas for HHMP-Si-CC system, there was a gradual decline of the DBC from top layer to bottom layer of PMMA rod because the concentration of the HHMP-Si-CC

decreased from top layer to bottom layer of PMMA rod. It is well known that DBC of methacrylate is closely related to the concentration of photoinitiator, and higher concentration of photoinitiator contributes to the improvement of DBC.

3.6. Molecular weight of gradient polymer

The radical photoinitiator concentration also significantly influences the polymer molecular weight that increases with the

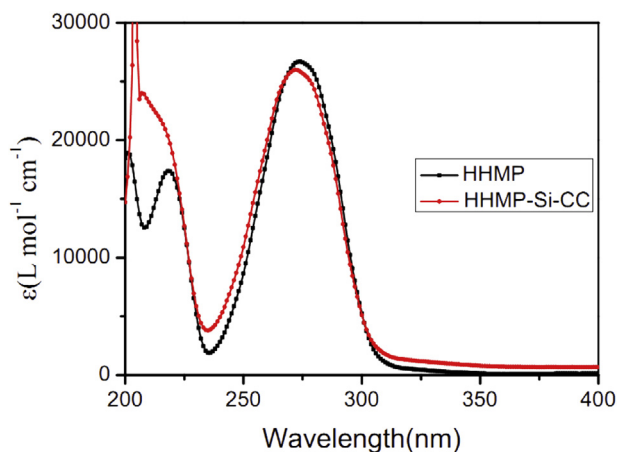


Fig. 3. UV-vis absorption spectra of HHMP and HHMP-Si-CC in absolute ethyl alcohol with the same molar concentration of chromophore (concentration = 2×10^{-4} mol L^{-1}).

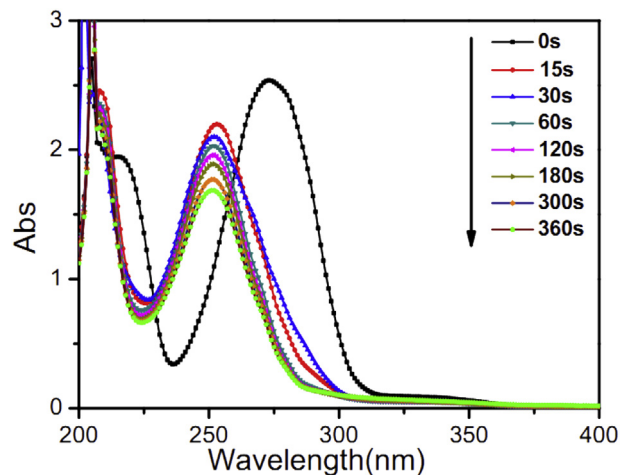


Fig. 4. UV-vis degradation curve of HHMP-Si-CC in absolute ethyl alcohol (concentration = 1×10^{-4} mol L^{-1}).

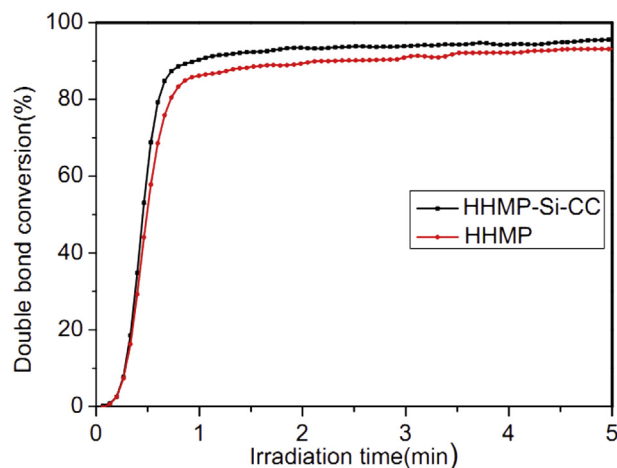


Fig. 5. Conversion versus time for the polymerization of TPGDA initiated by HHMP and HHMP-Si-CC with the same molar concentration of chromophore (concentration = $9 \times 10^{-3} \text{ mol L}^{-1}$).

decrease of photoinitiator concentration. The PMMA rod prepared using HHMP and HHMP-Si-CC respectively, as a photoinitiator, was cut into four small segments evenly to detect the effect of the gradient distribution of HHMP-Si-CC concentration on the molecular weight of the polymer. Fig. 11 shows that a progressive increase in the molecular weight for the PMMA rod initiated by HHMP-Si-CC from top to bottom layer. The result was attributed to the gradient distribution of concentration of HHMP-Si-CC. However, the molecular weight for the PMMA rod initiated by HHMP did not present an obviously gradient variation from top layer to bottom layer.

3.7. Thermostability and T_g of gradient polymer

Above research indicated that the gradient distribution of HHMP-Si-CC in the photopolymerization system resulted in the gradient distributions of degree of polymerization and molecular weight of PMMA initiated by HHMP-Si-CC, which would influence the thermostability and T_g of the polymer. The thermostability and T_g of the PMMA were therefore measured by thermal gravimetric analysis (TGA) and differential scanning calorimetry (DSC). It was observed from Table 2 that $T_{5\%}$ and T_{max} of the PMMA initiated by

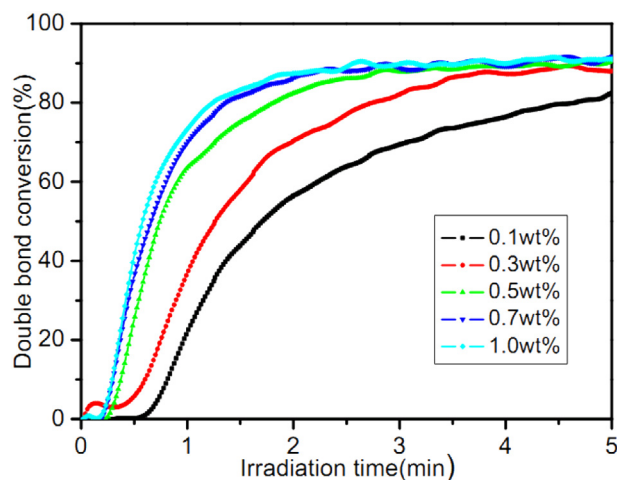


Fig. 6. Effect of the concentration of HHMP-Si-CC on the polymerization of TPGDA ($I = 40 \text{ mW cm}^{-2}$).

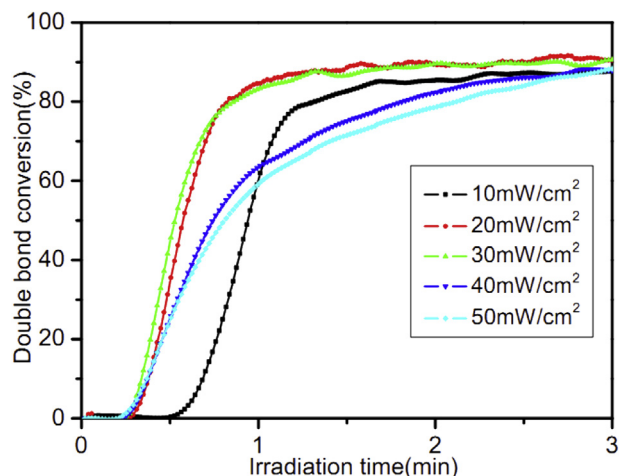


Fig. 7. Effect of the light intensity on the polymerization of TPGDA with 0.5 wt% HHMP-Si-CC.

HHMP-Si-CC gradually increased from top layer to bottom layer, indicating the gradual improvement of the thermal stability from top to bottom layer, while $T_{5\%}$ and T_{max} for PMMA initiated by HHMP presented an irregular change. This result was attributed to the progressive increase in the molecular weight for the PMMA rod initiated by HHMP-Si-CC from top to bottom layer. The increase of molecular weight of the polymer enhanced thermal stability of the polymer. It was also observed from Table 2 that the T_g decreased from the top layer to the bottom layer of PMMA initiated by HHMP-Si-CC, while the T_g of PMMA initiated by HHMP varied irregularly. This may be attributed to the decrease of the HHMP-Si-CC concentration from the top layer to the bottom layer of PMMA. In general, high photoinitiator concentration can increase the degree of branching of the polymer, while branching chains and acrylate pendant groups of PMMA are rigid groups, which confine the chain movement, thereby enhancing T_g .

3.8. Surface morphology of gradient polymer films

Oxygen inhibition is a commonly encountered issue while performing radical polymerizations. Many applications based on photopolymerizations namely paints, coatings, adhesives, photolithography, and dental resins are severely affected by oxygen

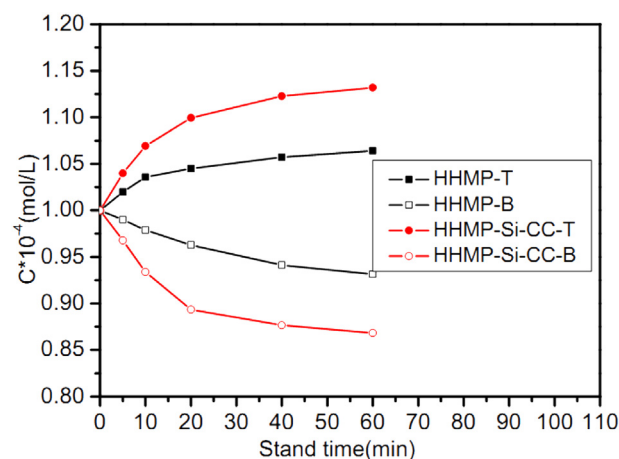


Fig. 8. The HHMP and HHMP-Si-CC concentrations of top and bottom layer of the system using absolute ethyl alcohol as a solvent with different standing time.

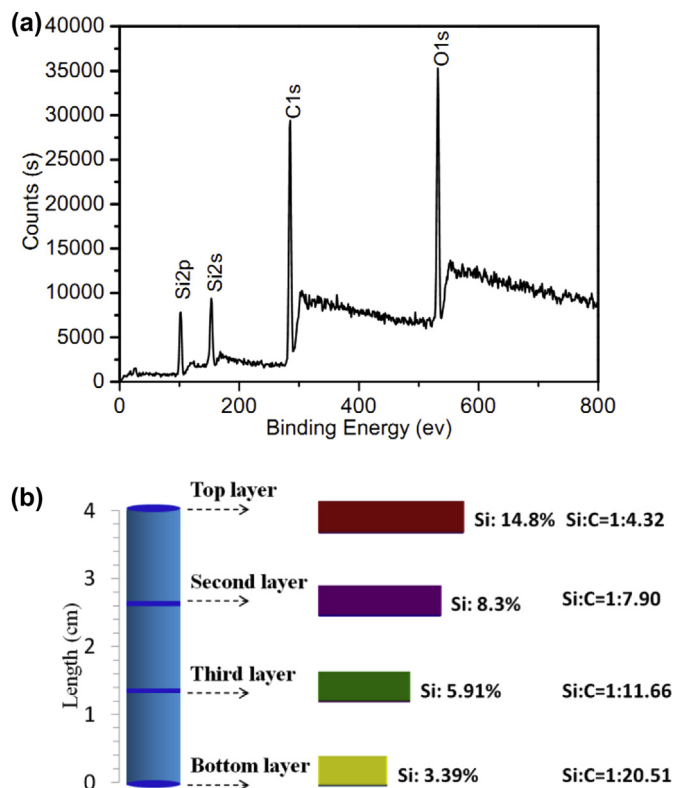


Fig. 9. (a) XPS survey spectrum of the polymer (PTPGDA) initiated by HHMP-Si-CC based on TPGDA; (b) Silicon content and atomic ratio of Si to C in each layer of the polymer.

inhibition. Currently, strategies to reduce oxygen inhibition are abundant, which include physical approaches such as nitrogen inerting, lamination and use of higher light intensity, as well as chemical strategies involving chemical additives [19–22], cationic polymerization [23], highly branched or multifunctional monomers, and acrylates with inherent reduced oxygen inhibition [24–25]. Among the chemical additive strategies, the most obvious method is to use a higher concentration of photoinitiator [26–27], which provides a higher concentration of initiating radicals. While the formed initiating radicals react more rapidly with molecular oxygen than with acrylate monomers, the concentration of oxygen within the system is initially decreased to a level that propagation becomes preferred [28]. The HHMP-Si-CC with self-floating ability can spontaneously enrich at the surface of the polymerization system, leading to a higher concentration of HHMP-Si-CC at the surface thereby decreasing oxygen inhibition. Here, we investigated the influence of oxygen inhibition in the photopolymerization systems initiated by HHMP and HHMP-Si-CC (Fig. 12).

When a liquid film of UV curable resin coated on a substrate is exposed to UV light in the presence of oxygen, a thin liquid layer of monomers remains uncured on the surface due to the quenching of free radicals by oxygen [29]. The uncured liquid layer could spontaneously swell the underlying substrate-constrained gradient polymer film, leading to in-plane stresses that generate surface wrinkle patterns [30]. Remarkably, the photopolymerization system initiated by HHMP in the presence of oxygen appeared a strong oxygen inhibition, while the oxygen inhibition was reduced to a certain extent by using the photoinitiator HHMP-Si-CC with self-floating ability (Fig. 12). Besides, it was observed from Fig. 13 that the wrinkling gradually became weak with the increase of the

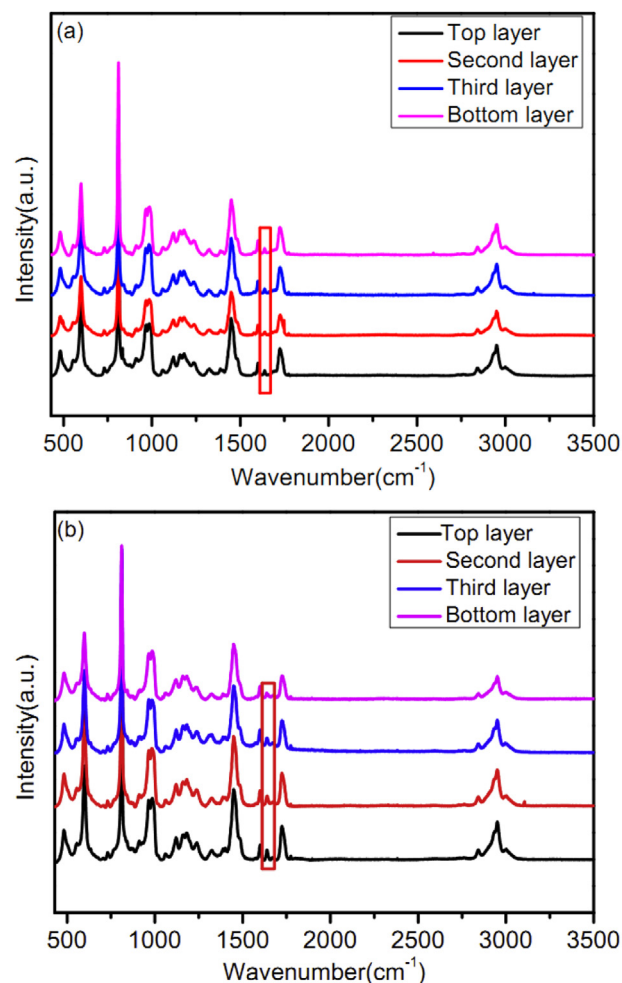


Fig. 10. Raman spectra of PMMA obtained by using HHMP (a) and HHMP-Si-CC (b) as photoinitiator ($1.0 \times 10^{-3} \text{ mol L}^{-1}$).

concentration of HHMP-Si-CC, and almost disappeared when the concentration of HHMP-Si-CC reached to $1.0 \times 10^{-2} \text{ mol L}^{-1}$, indicating that HHMP-Si-CC can reduce the oxygen inhibition through the enrichment on the surface of the photopolymerization system caused by the good self-floating ability.

3.9. Migration of photolysis fragments of photoinitiator from the cured material

To overcome the migration of photolysis fragments of the photoinitiator from UV-curable materials, the polymerizable groups were introduced into the HHMP-Si-CC molecule. The

Table 1
DBC of PMMA obtained by using HHMP and HHMP-Si-CC as photoinitiators ($1.0 \times 10^{-3} \text{ mol L}^{-1}$).

Photoinitiators	Segment	DBC(%)
HHMP	Top layer	97.23
	Second layer	97.43
	Third layer	98.02
	Bottom layer	97.33
HHMP-CC	Top layer	99.23
	Second layer	98.98
	Third layer	97.25
	Bottom layer	95.62

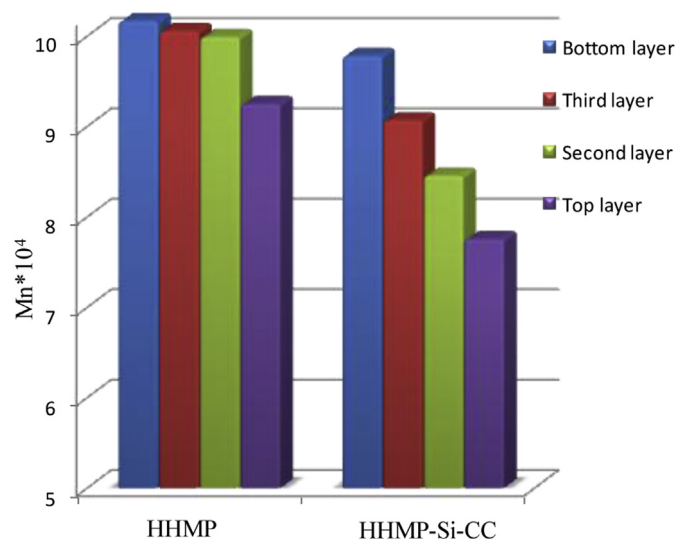


Fig. 11. Molecular weight of PMMA obtained by using HHMP and HHMP-Si-CC as photoinitiator ($1.0 \times 10^{-3} \text{ mol L}^{-1}$).

Table 2

Thermal decomposition parameters and T_g of each layer of PMMA prepared by using HHMP and HHMP-Si-CC as a photoinitiator.

Photoinitiators	Segments	$T_{5\%}/^\circ\text{C}$	$T_{\text{max}}/^\circ\text{C}$	$T_g/^\circ\text{C}$
HHMP	Top layer	188.2	384.2	111.4
	Second layer	188.5	382.6	115.7
	Third layer	189.5	382.5	115.5
	Bottom layer	188.8	386.8	113.6
HHMP-Si-CC	Top layer	158.4	370.4	118.2
	Second layer	188.2	387.2	116.8
	Third layer	191.5	390.5	115.9
	Bottom layer	237.7	395.7	111.2

Note: $T_{5\%}$ is the temperature of 5% weight loss. T_{max} is the peak temperature at maximum weight loss rate.

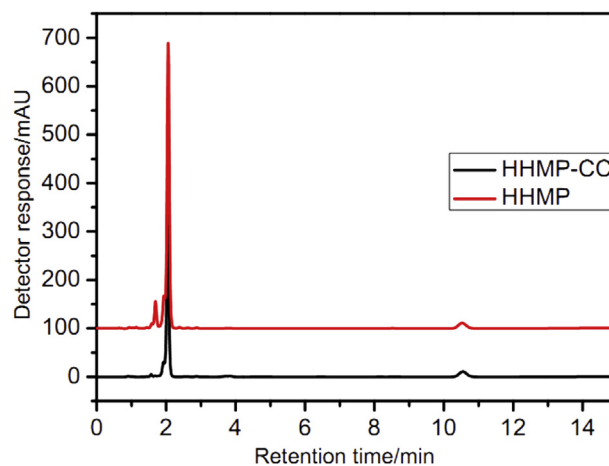


Fig. 14. HPLC chromatograms of extraction solutions of HHMP-Si-CC and HHMP.

photolysis fragments of HHMP-Si-CC can be polymerized into the polymer backbone through the carbon–carbon double bonds, thus, the migration of photolysis fragments from the cured material would be mitigated.

Here we investigated the migration of the photolysis fragments of the HHMP-Si-CC from UV-curable films by HPLC. The HPLC chromatograms of the extraction solution of the curable films initiated by HHMP-Si-CC and HHMP respectively (Fig. 14) showed that there were one intense peak at around 2.0 min and two small peaks at around 1.7 min and 10.5 min. The intense peak was assigned to the unreacted monomer TPGDA, while the small peak at around 10.5 min was assigned to the impurity in the solvent, the other small peak at around 1.7 min was the peak of photoinitiator fragments. Remarkably, the peaks of photoinitiator fragments and unreacted monomer TPGDA from the extraction solution of HHMP-Si-CC were obviously weaker than those of HHMP, demonstrating that HHMP-Si-CC with carbon–carbon double bonds prevented the migration of photolysis fragments from the cured material to some extent, and was an efficient photoinitiator.

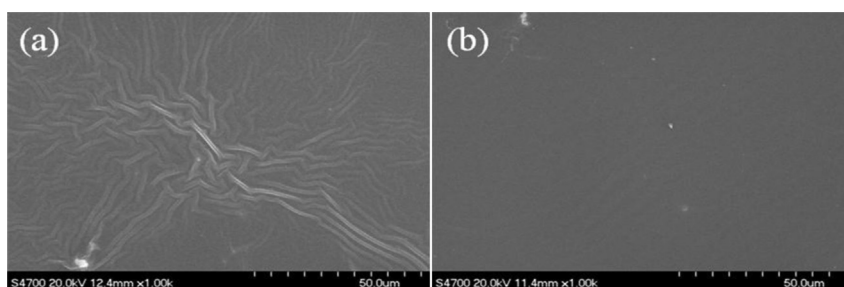


Fig. 12. SEM images of the polymer films (PTPGDA) initiated by HHMP and HHMP-Si-CC with the same molarity ($1.0 \times 10^{-2} \text{ mol L}^{-1}$).

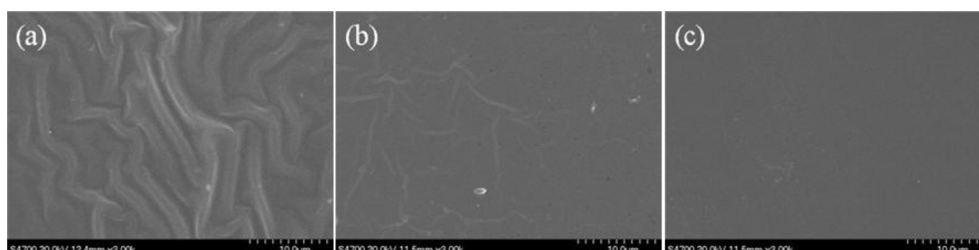


Fig. 13. SEM images of the polymer films (PTPGDA) initiated by different concentration of HHMP-Si-CC ((a) $4.0 \times 10^{-3} \text{ mol L}^{-1}$ (b) $8.0 \times 10^{-3} \text{ mol L}^{-1}$ (c) $1.0 \times 10^{-2} \text{ mol L}^{-1}$).

4. Conclusions

In this paper, a novel photocleavage polysiloxane macromolecular photoinitiator with polymerizable group (HHMP-Si-CC) was synthesized, and its structure was confirmed by ^1H NMR, FTIR and GPC. The UV absorption spectra showed that HHMP-Si-CC had a maximum absorption peak at 275 nm and its intensity decreased with the increase of the irradiation time. The kinetics of photopolymerization and SEM images of curable films initiated by HHMP-Si-CC indicated that HHMP-Si-CC efficiently initiated photopolymerization and mitigated the oxygen inhibition in radical photopolymerization to a certain degree.

The UV absorption spectra and XPS proved that the HHMP-Si-CC had relatively good self-floating ability and spontaneously formed a gradient distribution of concentration in the polymerization system after standing for a designated time. The polymer initiated by HHMP-Si-CC presented a gradient change in the degree of polymerization, molecular weight, thermostability and T_g , indicating that gradient polymeric material was obtained by using the photoinitiator HHMP-Si-CC under irradiation of UV light. More importantly, HPLC chromatograms demonstrated that the migration of photolysis fragments of HHMP-Si-CC with polymerizable groups toward the cured material surface was mitigated significantly. The HHMP-Si-CC should have potential applications in preparing more environmentally friendly gradient materials.

Acknowledgements

The financial support from National Natural Science Foundation of China (Grant No. 51273014) is gratefully acknowledged.

Appendix A. Supplementary data

Supplementary data related to this article can be found at <http://dx.doi.org/10.1016/j.polymer.2014.06.040>.

References

- [1] Zhang Y. *J Eur Ceram Soc* 2012;32:2623–32.
- [2] Wen B, Wu G, Yu J. *Polymer* 2004;45:3359–65.
- [3] Bhat RR, Chaney BN, Rowley J, Liebmann-Vinson A, Genzer J. *Adv Mater* 2005;17:2802–7.
- [4] Kim J, Mok MM, Sandoval RW, Woo DJ, Torkelson JM. *Macromolecules* 2006;39:6152–60.
- [5] Gritsenko KP, Krasovsky AM. *Chem Rev* 2003;103:3607–49.
- [6] Cui Y, Yang J, Zeng Z, Chen Y. *Eur Polym J* 2007;43:3912–22.
- [7] Yao D, Zhang W, Zhou JG. *Biomacromolecules* 2009;10:1282–6.
- [8] Jiang D, Huang X, Qiu F, Luo C, Huang LL. *Macromolecules* 2010;43:71–6.
- [9] Song C, Xu Z, Li J. *Mater Des* 2007;28:1012–5.
- [10] Zhang N, Li M, Nie J, Sun F. *J Mater Chem* 2012;22:9166–72.
- [11] Liska R. *J Polym Sci Part A: Polym Chem* 2002;40:1504–18.
- [12] Teshima W, Nomura Y, Tanaka N, Urabe H, Okazaki M, Nahara Y. *Biomaterials* 2003;24:2097–103.
- [13] Tar H, Esen DS, Aydin M, Ley C, Arsu N. *Macromolecules* 2013;46:3266–72.
- [14] Kitano H, Ramachandran K, Bowden N, Scranton AJ. *Appl Polym Sci* 2013;128:611–8.
- [15] Wang H, Wei J, Jiang X, Yin J. *J Polym Sci Part A: Polym Chem* 2006;44:3738–50.
- [16] Yagci Y, Jockusch S, Turro NJ. *Macromolecules* 2010;43:6245–60.
- [17] Hou G, Shi S, Liu S. *Polym J* 2008;40:228–32.
- [18] Fu H, Zhang S, Xu T, Zhu Y, Chen J. *Environ Sci Technol* 2008;42:2085–91.
- [19] Ibrahim A, Stefano LD, Tarzi O, Tar H, Ley C, Allonas X. *Photochem Photobiol* 2013;89:1283–90.
- [20] Tejkl M, Vališ J, Kaplanová M, Jašúrek B, Syrový T. *Prog Org Coat* 2012;74:215–20.
- [21] Roper TM, Kwee T, Lee TY, Guymon CA, Hoyle CE. *Polymer* 2004;45:2921–9.
- [22] Versace DL, Dalmas F, Fouassier JP, Lalevee J, Dichloride Z. *Macro Lett* 2013;2:341–5.
- [23] Crivello JV, Ma J, Jiang F, Hua H, Ahn J, Ortiz RA. *Macromol Symp* 2004;215:165–78.
- [24] Cai Y, Jessop JLP. *Polymer* 2006;47:6560–6.
- [25] Decker C, Viet TNT, Decker D, Weber-Koehl E. *Polymer* 2001;42:5531–41.
- [26] Hageman HJ. *Prog Org Coat* 1985;13:123–50.
- [27] Hageman HJ, Jansen LGJ. *Makromol Chem* 1988;189:2781–95.
- [28] Ligon SC, Husar B, Wutzel H, Holman R, Liska R. *Chem Rev* 2014;114:557–89.
- [29] Lalevée J, Fouassier JP. *Polym Chem* 2011;2:1107–13.
- [30] Chandra D, Crosby AJ. *Adv Mater* 2011;23:3441–5.